Ageing effect on cyclic plasticity of a tempered martensitic steel

Z. Zhang, Denis Delagnes, Gérard Bernhart

Ageing effect on cyclic plasticity of a tempered martensitic steel

Z. Zhang [a,*], D. Delagnes [b], G. Bernhart [b]

[a] Electromechanics and Materials Engineering College, Dalian Maritime University, Dalian 116026, China
[b] Research Centre on Tools, Materials and Processes (CROMeP), Ecole des Mines d'Albi-Carmaux, 81013 Albi CT cedex 09, France

Abstract

Specific isothermal cyclic deformation tests were carried out on a tempered martensitic steel 55NiCrMoV7 at four hardness levels in the temperature range 20–600 °C. The cyclic stress response generally shows an initial exponential softening for the first few cycles, followed by a gradual softening without saturation. The influences of initial hardness obtained after tempering, temperature, strain rate and ageing on cyclic plasticity are discussed by means of hardness measurements and equivalent ageing experiments. Compared to hardness measured after ageing without fatigue loading, hardness dramatically decreases when the specimen is simultaneously subjected to ageing and fatigue at elevated temperature. Cyclic softening intensity increases with testing temperature from 300 to 600 °C, but the maximal softening intensity occurs at room temperature. This is inconsistent with hardness measurements performed on the specimen after a fatigue test conducted at room temperature. The final discussion focuses on the mechanisms involved in the softening of martensitic steels to explain the last result.

Keywords: Martensitic steel; Hardness measurements; Cyclic softening; Plasticity; Ageing; Tempering ratio

1. Introduction

Hot-work tool steels are widely used at various tempering conditions to obtain the mechanical properties requested by the industrial application, like hot forging, casting, hot-rolling, extrusion, where the steel endures thermal and mechanical cyclic loads [1]. In addition to wear and abrasion, most of the investigations indicate that cyclic plasticity is responsible for limited tool lifetime [2,3]. Nevertheless, fatigue behaviour of steels not only depends upon the testing conditions such as temperature, frequency, strain amplitude, stress ratio, etc., but also upon microstructure obtained after heat treatment in industrial conditions. Tempering is the last treatment required before the martensitic steel can be used. The tempering process can be considered as a phase transformation promoted by diffusion from an unstable state (martensite) towards a stable equilibrium state (ferrite + globular carbides), which corresponds to the annealed state of steel. The tempered steel is therefore in a quasi equilibrium state (ferrite + primary carbides and small secondary carbides) which is supposed to evolve towards a stable equilibrium state as long as thermal and mechanical conditions allow the evolution of the microstructure involved in the tempering process (coalescence of carbides, arrangement of the dislocation structure).

Furthermore, some investigations [4,5] have shown that temperature measured at the die surface exceeds the tempering temperature of the steel during one working turn. In such conditions, the steel is subjected to a continuous evolution of microstructure and mechanical properties during service life. It is therefore of great importance to derive an anisothermal constitutive model, which may be able to take into account the large range of strain rates, the temperature variations as well as the effect of ageing. The ultimate aim of such an approach, which

* Corresponding author. Tel./fax: +86 411 84725568.
E-mail address: zzp@newmail.dlmu.edu.cn (Z. Zhang).

consists in taking into account interactions between microstructure and properties, is to ensure a good prediction of fatigue behaviour in order to optimise tool design and to derive a more realistic life prediction model. To reach this goal, some models were derived over recent years in the case of stable microstructures [6–9]. The study of microstructural evolutions during tempering at different scales (ex-austenitic grains, martensitic laths and carbides) was reported in a previous paper [10]. The definition of a tempering ratio based on hardness measurements was proposed and a tempering kinetic law was derived in the form of the Johnson–Mehl–Avrami equation. Moreover, an anisothermal cyclic behaviour model that takes into account the tempering effect of a martensitic tool steel was proposed by Zhang et al. [11,12]. Hardness tests are widely used in quality control, design, alloy development and materials selection. This measurement of the resistance to penetration is often linked to both yield and tensile strength with empirical relationships. Recently, several authors investigated the relationship between cyclic behaviour and hardness measured after fatigue [13–15]. This led to the conclusion that hardness measurement can be a relevant test to evaluate cyclic hardening or softening and even fatigue damage. However, those investigations were limited to a single testing temperature and tempered state.

The aim of the present study is to investigate the influence of the tempering treatment on the cyclic behaviour of a martensitic steel. In addition, the effects of ageing, testing temperature and strain rate on cyclic behaviour for various tempered conditions are discussed. The relationship between the decrease in hardness and the cyclic softening intensity is also investigated and discussed from room temperature up to 600 °C which is the highest tempering temperature.

2. Experimental procedures

2.1. Material and heat treatment

The steel investigated is a 55NiCrMoV7 hot-work tool steel with the following chemical composition (wt%): 0.56C, 1.7Ni, 1.0Cr, 0.5Mo, 0.1V, 0.2Si and 0.7Mn. In order to investigate the effect of tempering on the cyclic behaviour, samples were manufactured with four different hardnesses corresponding to the usual states required for industrial applications. Quenching and tempering conditions as well as measured Vickers hardness are reported in Table 1. The microstructure was investigated by Scanning Electron Microscopy (SEM, PHILIPS-XL30). Hardness measurements were performed using a Buehler® MICROMET® 2001 type microhardness tester. Thirty indentations with 0.2 kg load were performed on each sample. The standard deviation is approximately 10 Vickers ($HV_{0.2}$). The mean values were considered as the hardness results reported.

Table 1
Heat-treatment conditions and corresponding hardness for the 55NiCrMoV7 steel

Tempering temperature (°C)	Tempering time (h)	Vickers hardness ($HV_{0.2}$)
350	2	580
460	2	509
560	2	457
600	2	376

Quenching condition: austenitisation at 850 °C for 1 h, quenching in vacuum.

2.2. Fatigue tests

For each tempering state defined in Table 1, total strain controlled fatigue tests were performed at the following temperatures: 20 °C (room temperature), 300, 400, 500 and 600 °C. Fatigue tests were carried out with a closed-loop MTS 810 servo-hydraulic testing machine and Teststar II™ controller connected to a personal computer. Cylindrical 180 mm long fatigue testing samples with a gauge diameter of 5 mm and a gauge length of 16 mm were mounted in water-cooled grips. The specimen surface was polished with silicon carbide paper down to 1200 grit. Heating was achieved with a 6-kW induction generator. Strain is recorded with a 12-mm gauge length contact extensometer equipped with alumina rods. Temperature was controlled on the middle of the sample by mechanically applied thermocouples [9]. Cyclic tests were started after heating the specimen at a rate of 200 °C/min and a temperature stabilisation period of 75 s. Fig. 1 identifies several relevant points of the fatigue experiment used later in the discussion.

Fatigue tests were performed in reversed total strain amplitude conditions with a triangular waveform. All the tests were performed with fixed total strain amplitude of ±0.8%. Strain rate is kept constant at $10^{-2}\,s^{-1}$ during the first phase. The number of cycles defining the first phase

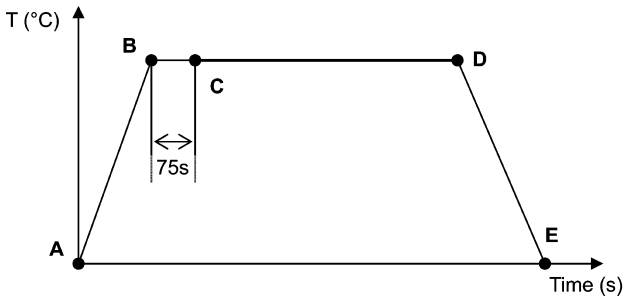

Point A: initial state (as tempered state)
Point C: state after heating and before cycling
Point E: final state after fatigue test
Section B – C: stabilisation duration at testing temperature before cycling
Section C – D: duration of fatigue cycling

Fig. 1. Different stages of a fatigue test.

was selected in order to reach a near constant cumulative plastic strain (p) close to 4 mm/mm whatever the testing temperature and hardness of the sample. Then, strain rate is changed to 10^{-3}, $10^{-4}\,s^{-1}$ and finally returned to $10^{-2}\,s^{-1}$. Only three cycles were performed at each strain rate during this second phase. More details on the experimental procedure can be found in [7]. The strain rates were selected to cover the industrial strain rate conditions arising when forging dies are used in mechanical or hydraulic presses.

3. Experimental results

3.1. Cyclic softening

The typical cyclic behaviour of the 55NiCrMoV7 steel is shown in Fig. 2 where the stress amplitude is plotted against the number of cycles for each hardness level. The quenched and tempered 55NiCrMoV7 steel undergoes cyclic softening for each initial hardness and testing temperature, i.e. stress amplitude decreases with the number of cycles. This softening can be divided into two phases, which are the sharp softening phase during the initial few hundred cycles and the slow softening phase throughout the greater part of the lifetime [1,3]. The former is generally explained by the rapid change of dislocation density and structure and the latter is related to both the modification of dislocation sub-structure and the dynamic coalescence of carbides [12,17,18]. Fig. 2 shows that cyclic softening is strongly influenced by both testing temperature and initial hardness.

Fig. 3 shows the evolution of the stress amplitude according to the number of cycles for each testing temperature investigated. At 20 and 300 °C (Fig. 3a and b), the stress amplitudes are clearly separated for the different hardness levels, i.e. stress amplitude increases when hardness increases, whereas for higher testing temperatures, the fatigue behaviour may be very close for two or more different initial hardness. This is particularly evident for 580HV and 509HV samples at 500 and 600 °C (Fig. 3d and e). This particular phenomenon is discussed in the following section.

Previous work [1,6–9] has shown that cyclic behaviour could be described using a cyclic constitutive model expressed under the classical framework of thermodynamics of irreversible processes. In such models, the cyclic behaviour of the steel can be described as a function of the cumulative plastic strain rather than the number of cycles. Consequently, the softening intensity is defined by the difference between the maximum stress amplitude measured at the first cycle and the stress amplitude measured at cumulative plastic strain $p = 4$: $(\Delta\sigma/2)_{max} - (\Delta\sigma/2)_{p=4}$. Results are reported in Table 2 for every considered initial hardness at each temperature. The softening intensity increases with testing temperature from 300 to 600 °C, except for the highest hardness level. The softening intensity is as high as 200 MPa at 600 °C for the sample with initial hardness of 457HV. However, the maximum softening intensity is measured at 20 °C for each hardness.

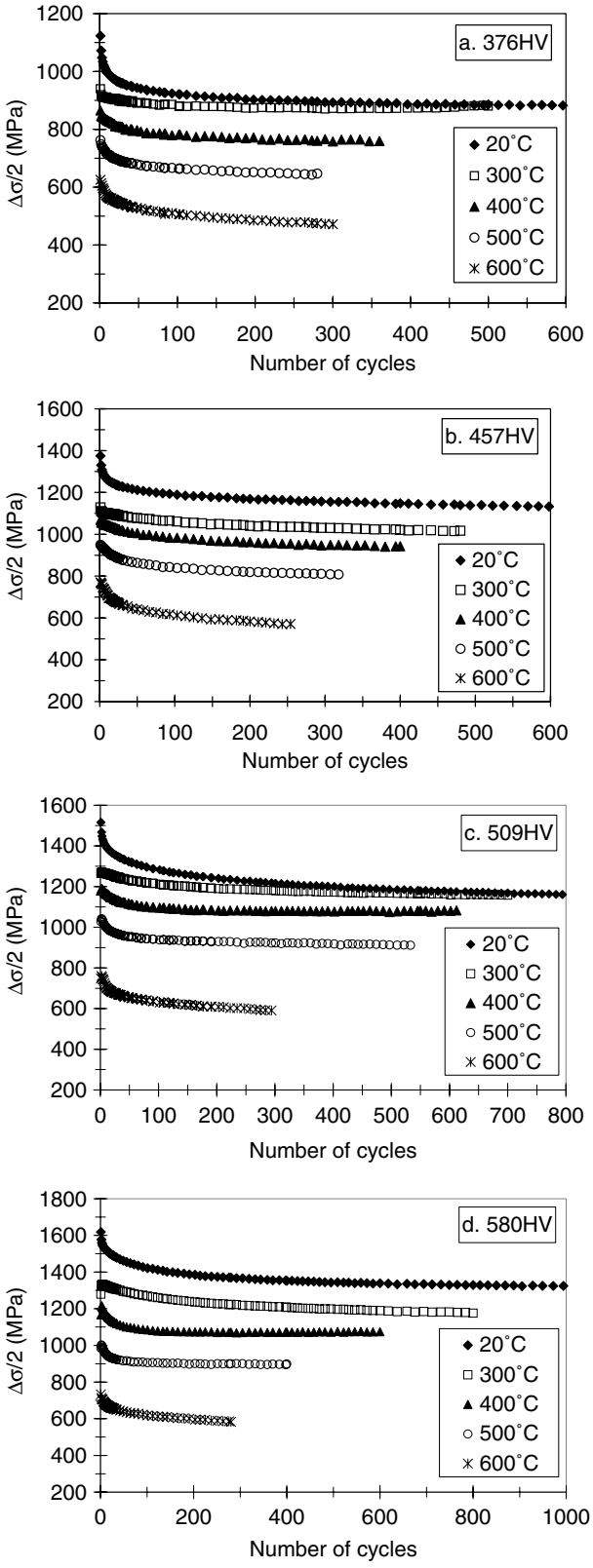

Fig. 2. Stress amplitude according to number of cycles for initial hardness from 376HV (a) to 580HV (d); Other conditions are $\Delta\varepsilon_t = \pm 0.8\%$ and strain rate $= 10^{-2}\,s^{-1}$.

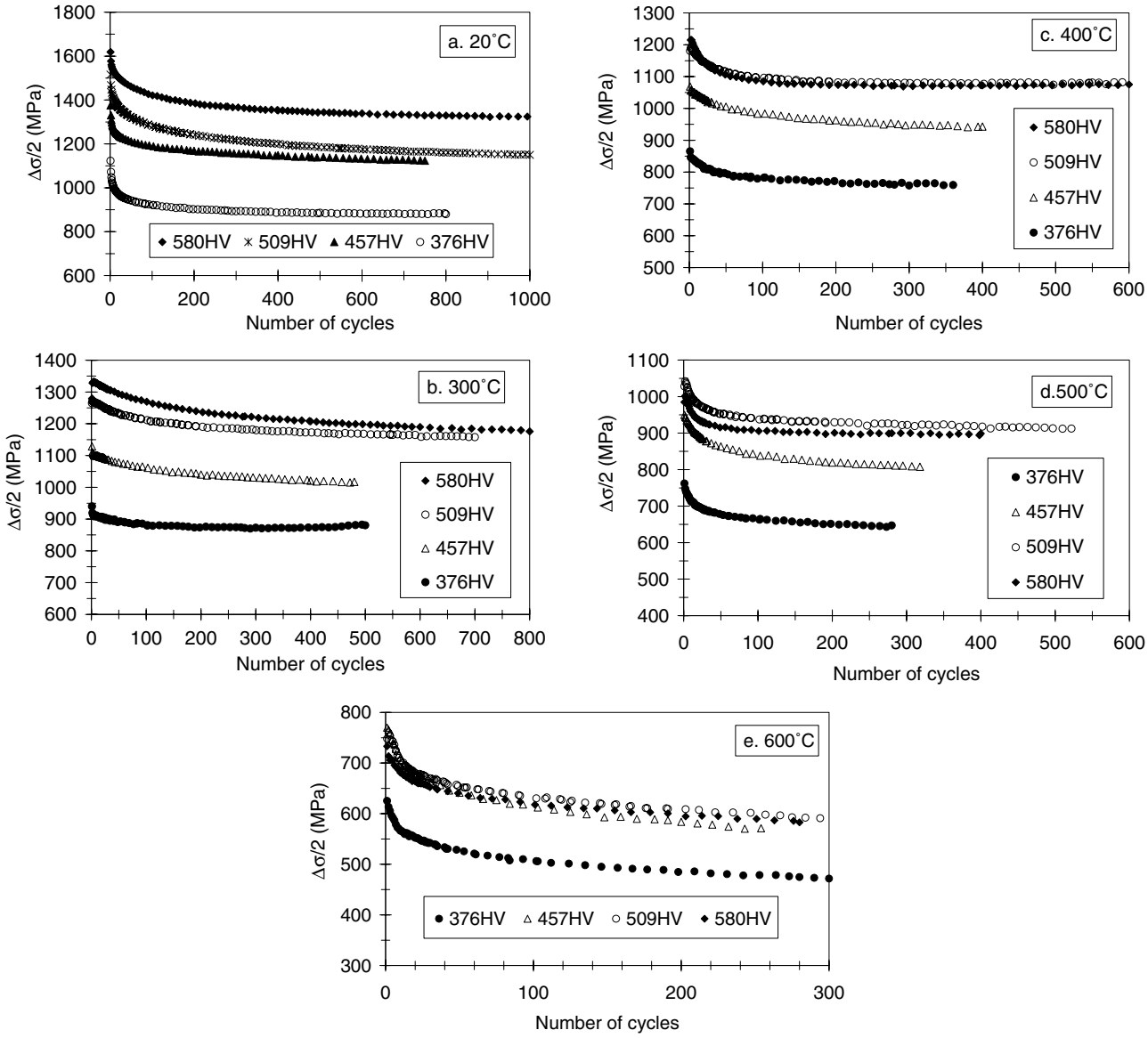

Fig. 3. Stress amplitude according to number of cycles for increasing testing temperatures: 20 °C (a), 300 °C (b), 400 °C (c), 500 °C (d), 600 °C (e).

Table 2
Softening intensity measured at $p = 4$ for every conditions of testing temperature and initial hardness

	Cyclic softening intensity (MPa)			
	376HV	457HV	509HV	580HV
Testing temperature (°C)				
20	243	252	366	298
300	60	112	113	157
400	106	126	110	140
500	115	143	140	103
600	154	200	170	150

3.2. Maximum stress

Fig. 4 presents the relationship of the maximum stress (measured at $\varepsilon_t = 0.8\%$ during the first loading) to testing temperature. For each hardness level, maximum stress decreases with the testing temperature. Moreover, for the highest temperature, the maximum stress tends to be similar for each hardness. As shown in Fig. 5 presenting the evolution of the maximum stress with the difference between fatigue temperature (T_f) and tempering temperature (T_t), the figure can be divided into two parts. On the left, the maximum stress linearly decreases with temperature difference for each level of hardness. When temperature difference is positive (above the tempering temperature), the maximum stress intensively decreases; probably due to the rapid evolution of the microstructure (recovery and carbides coalescence) which is enhanced by thermal ageing effect.

3.3. Strain rate

Considering the second phase of the fatigue experiments (three cycles at strain rates respectively equal to 10^{-2}, 10^{-3}

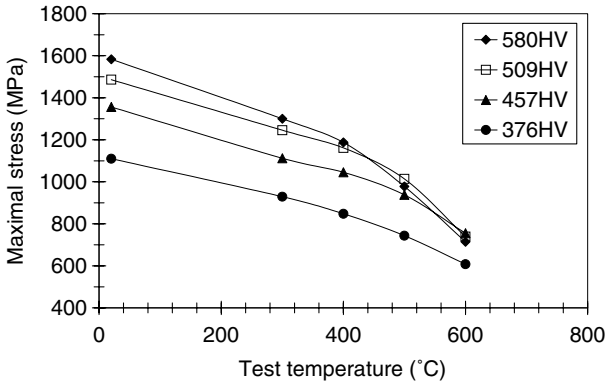

Fig. 4. Maximum stress measured at the first cycle according to the testing temperature.

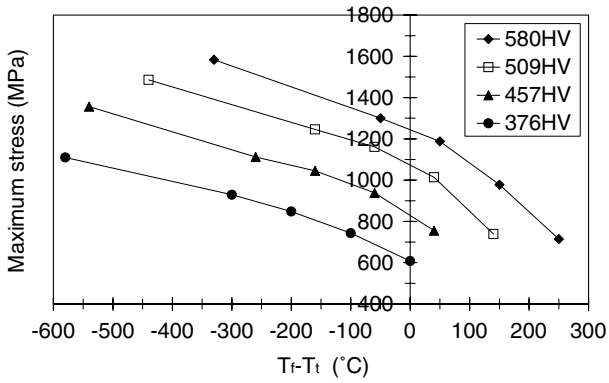

Fig. 5. Maximum stress measured at the first cycle according to the difference between testing temperature (T_f) and tempering temperature (T_t).

and $10^{-4}\,s^{-1}$), the effects of strain rate were investigated from 20 to 600 °C. The stress amplitudes measured at the second cycle are reported in Table 3.

The effect of strain rate on stress–strain hysteresis loops is shown in Fig. 6 for 376HV (400 and 600 °C) and 457HV (20 and 600 °C). Analysing Table 3 and Fig. 6, results show that hysteresis loops are similar for the three strain rates at temperatures lower than 400 °C (see Fig. 6a and b). At higher testing temperatures ($T \geqslant 500$ °C), influence of strain rate becomes more and more important as shown in Fig. 6c and d at 600 °C. The difference in stress amplitude reaches 200 MPa at 600 °C for a 376HV sample (Fig. 6d and Table 3).

The strain rate effect can be appreciated defining a relative factor F as a ratio between the stress amplitude for the 10^{-2} or $10^{-3}\,s^{-1}$ strain rate to that of the slowest rate ($10^{-4}\,s^{-1}$):

$$F_{2/4} = (\Delta\sigma)_{\dot{\varepsilon}=10^{-2}}/(\Delta\sigma)_{\dot{\varepsilon}=10^{-4}} \quad \text{and}$$
$$F_{3/4} = (\Delta\sigma)_{\dot{\varepsilon}=10^{-3}}/(\Delta\sigma)_{\dot{\varepsilon}=10^{-4}}. \tag{1}$$

Evolutions of $F_{2/4}$ and $F_{3/4}$ with testing temperature are shown Fig. 7. $F_{2/4}$ and $F_{3/4}$ values remain nearly constant and close to 1 from 20 to 400 °C. Therefore, the cyclic behaviour can be considered as independent of strain rate for this temperature range. Conversely, a huge strain rate effect is observed for testing temperatures above 500 °C. Indeed, the stress amplitude measured for a strain rate of $10^{-2}\,s^{-1}$ is nearly 1.5 times higher than the stress amplitude for a strain rate of $10^{-4}\,s^{-1}$ (Fig. 7). Consequently, it is of primary importance to take into account the strain rate effect [19,20] for usual industrial applications of hot-work tool steels.

4. Discussion

A tempering treatment is required to increase the ductility of the steel after quenching. Such a tempering process can be considered as a phase transformation promoted by diffusion from an unstable state (martensite = carbon supersaturated quadratic structure: maximum hardness) towards a stable equilibrium state (body centred cubic structure α-Fe + large globular carbides: lowest hardness), which corresponds to the annealed state. Quenched and tempered steel move towards a stable equilibrium state as long as favourable conditions of time and temperature are applied. In general, hardness cannot be clearly related to the softening state between the quenched and equilibrium state. Consequently, a definition of a tempering ratio (τ_v), based on the measurement of hardness of the steel, was introduced in a previous work [10], as follows:

$$\tau_v = \frac{H_v - H_0}{H_\infty - H_0}, \tag{2}$$

where H_0 is the hardness after quenching, H_∞ is the hardness in the annealed state, and H_v is the hardness obtained

Table 3
Influence of the strain rate on the stress amplitude measured at the second cycle

	Stress amplitude (MPa)											
Hardness:	376HV			457HV			509HV			580HV		
Strain rate (s^{-1}):	10^{-2}	10^{-3}	10^{-4}	10^{-2}	10^{-3}	10^{-4}	10^{-2}	10^{-3}	10^{-4}	10^{-2}	10^{-3}	10^{-4}
Testing temperature (°C)												
20	885	884	879	1131	1125	1124	1154	1142	1151	1341	1320	1339
300	881	875	858	1014	1015	1006	1155	1143	1133	1171	1156	1145
400	762	751	745	942	933	925	1075	1070	1055	1074	1061	1044
500	631	632	604	806	786	755	905	873	804	884	857	780
600	471	414	340	555	499	410	583	509	409	580	504	404

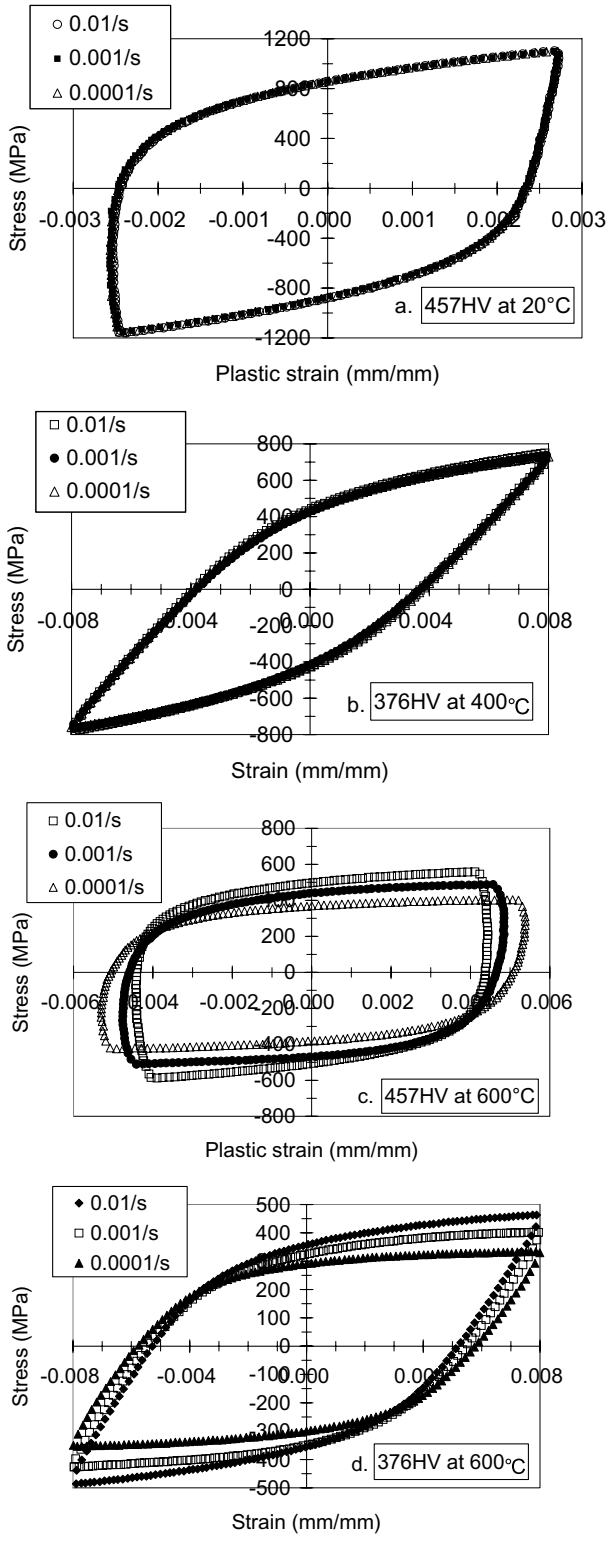

Fig. 6. Influence of strain rate on the stress-plastic strain loop at: (a) 20 °C (HV = 457), (b) 400 °C (HV = 376), (c) 600 °C (HV = 457), (d) 600 °C (HV = 376).

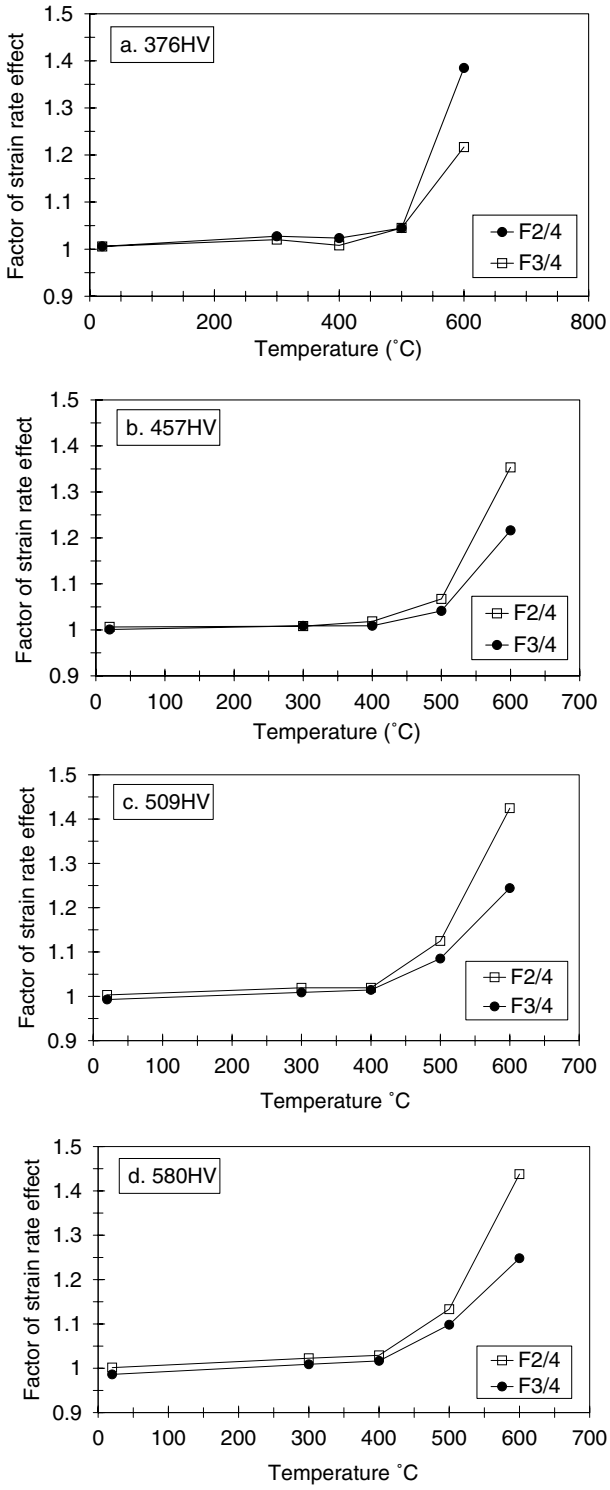

Fig. 7. Factor of strain rate effect vs. testing temperature for initial hardness from 376HV (a) to 580HV (d).

after a standard tempering. According to this definition, tempering ratio values fall between 0 (as-quenched state) and 1 (annealed state). From this definition, a tempering kinetic law was proposed in the form of the Johnson–Mehl–Avrami type equation as follows:

$$\tau_v = 1 - \exp(-(D \cdot t)^m), \tag{3}$$

where t is the tempering time, m is the ageing exponent depending on the material and the previous heat treatment.

D depends on tempering temperature and follows the Arrhenius equation:

$$D = D_0 \exp\left(-\frac{Q}{RT}\right), \tag{4}$$

where D_0 is the pre-exponential constant, Q is the activation energy of the tempering transformation, R is the perfect gas constant (equal to 8.31 J K^{-1} mol^{-1}) and T is the tempering temperature in Kelvin.

Combining Eqs. (2) and (3), the tempering hardness can be expressed by the following equation:

$$H_v = H_\infty + (H_0 - H_\infty) \cdot \exp(-(D \cdot t)^m). \tag{5}$$

All parameters (Table 4) can be determined measuring hardness levels for as-quenched, as-annealed and various tempered conditions performed at different temperatures and durations.

Table 4
Parameters of the tempering kinetic law for the steel 55NiCrMoV7 [11]

Parameter	H_0 ($HV_{0.2}$)	H_∞ ($HV_{0.2}$)	D_0 (s^{-1})	Q (kJ mol^{-1})	m
Value	776	210	2.7×108	231	0.0518

In Section 3.1, unusual cyclic behaviours were pointed out. In other words, the stress response of some specimens with higher hardness is even lower than specimens with lower hardness. In order to investigate this particular phenomenon, the hardness of the specimens after fatigue was measured on the section surface in the middle of the 12-mm gauge length after polishing. Hardness results are reported in Table 5. The tempering ratio of specimens was calculated using Eq. (2) both after tempering and after fatigue test. As it is experimentally impossible to access the hardness of samples at high temperatures and during the fatigue testing, the tempering kinetic law (Eq. (3)) was used to calculate tempering ratios of specimens before and after cycling. These calculated values permit to evaluate the decrease in hardness induced by the thermal ageing only. The calculated values of hardness and tempering ratio are shown in Table 5.

In comparison with the as-tempered state, specimen hardness appreciably decrease during the cyclic test. Results are reported in Fig. 8 where the reduction in hardness during fatigue ($H_t - H_f$) is plotted with respect to the testing temperature (H_t: measured hardness after tempering, H_f: measured hardness after fatigue testing). Increasing

Table 5
Experimental and calculated hardness and tempering ratios

Testing temperature (°C)	Tempering temperature (°C)							
	600	560	460	350	600	560	460	350
	Measured hardness of tempered steel (H_t) at point A				Experimental tempering ratio after tempering using Eq. (2)			
20	374	457	505	570	0.7102	0.5636	0.4788	0.3640
300	372	453	506	581	0.7138	0.5707	0.4770	0.3445
400	380	457	504	580	0.6996	0.5636	0.4806	0.3463
500	374	464	511	584	0.7103	0.5512	0.4682	0.3392
600	378	453	518	584	0.7031	0.5707	0.4558	0.3392
	Calculated hardness before cycling at point C using Eq. (5)				Calculated tempering ratio before cycling at point C using Eq. (3)			
20	374	457	505	570	0.7102	0.5636	0.4788	0.3640
300	372	453	506	581	0.7138	0.5707	0.4770	0.3445
400	380	457	504	***578***	0.6996	0.5636	0.4806	**0.3507**
500	374	464	511	***543***	0.7102	0.5512	**0.4688**	**0.4123**
600	378	453	***501***	***503***	0.7031	**0.5708**	**0.4855**	**0.4820**
	Calculated hardness after fatigue at point D using Eq. (5)				Calculated tempering ratio after fatigue at point D using Eq. (3)			
20	374	457	505	570	0.7102	0.5636	0.4788	0.3640
300	372	453	506	581	0.7138	0.5707	0.4770	**0.3448**
400	380	457	504	***553***	0.6996	0.5636	**0.4807**	**0.3943**
500	374	464	***499***	***504***	0.7102	**0.5516**	**0.4888**	**0.4803**
600	378	***450***	***463***	***464***	**0.7032**	**0.5767**	**0.5528**	**0.5520**
	Measured hardness after fatigue (H_f)				Experimental tempering ratio after fatigue test using Eq. (2)			
20	365	450	496	560	0.7261	0.5760	0.4947	0.3816
300	361	441	494	517	0.7332	0.5919	0.4982	**0.4576**
400	359	432	488	***491***	0.7367	0.6078	**0.5088**	**0.5035**
500	338	420	***447***	***442***	0.7739	**0.6290**	**0.5813**	**0.5901**
600	329	***397***	***391***	***359***	**0.7898**	**0.6696**	**0.6802**	**0.7367**

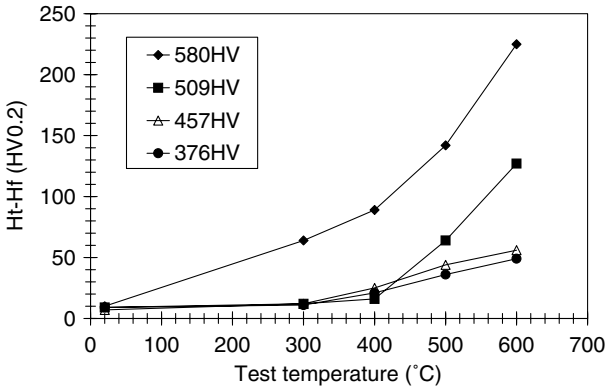

Fig. 8. Decrease in hardness during fatigue testing at various temperatures.

the initial hardness and the testing temperature induces a decrease in hardness during fatigue. Fig. 9 presents the reduction in hardness during cycling against the difference between the fatigue amtemperature (T_f) and tempering temperature (T_t). Results can be summarised as follows:

(i) if testing temperature is lower than the tempering temperature, reduction in hardness is limited whatever the initial hardness;
(ii) on the contrary, the hardness sharply decreases when the temperature difference is positive. The reduction reaches 225HV for the 580HV sample tested at 600 °C, i.e. hardness after testing is about 60% of the initial hardness. Results clearly shows that fatigue testing at high temperature strongly influences the ageing of the steel;

The hardness measurement is a compression test with a calculated average strain above 10%. This is an easy way to evaluate the resistance to plastic deformation and mechanical strength. Indeed, relationships between hardness and both tensile and yield strength can be found in the literature. More recently, different authors have investigated relationships between cyclic behaviour and hardness change during fatigue [13–15]. In addition, fatigue behaviour and even fatigue damage were evaluated using hardness measurements [15,16]. When quenched and tempered steels are subjected to strain controlled fatigue, a sharp cyclic softening is obtained as shown in Figs. 2 and 3. Generally, each performed test shows both cyclic softening (stress amplitude decrease) and reduction in hardness during low cycle fatigue. This result is in agreement with the work performed by Okazaki et al. [13]: materials presenting a cyclic softening also show a decrease of hardness. The results obtained by Okamura et al. [14] on a 9Cr–1Mo steel also showed hardness decrease during fatigue, but the investigation was limited to a single testing temperature. In the present study, investigations were conducted at different temperatures for four tempered states. Results show that reduction in hardness rises with the testing temperature for each tempered state. Conversely, cyclic softening intensity presents a more complex relation with the testing temperature as shown in Fig. 10. Indeed, at room temperature, a maximum value of softening intensity is measured for each initial hardness. At 300 °C, the softening intensity is reduced to its lowest value. An increase with the testing temperature is observed above 300 °C. As has been already shown and precisely described by several authors, the cyclic softening is first explained by a strong decrease of the dislocation density generated during the quench [21,22,24] and a subsequent modification of the dislocation structure [25–29]. The second mechanism involved in the softening is the coalescence of precipitates [23,24] which also modifies the free slip distances of dislocations. This second mechanism is obviously thermally activated and moreover, the secondary carbides coalescence is clearly accelerated under fatigue at elevated temperature. Such dynamic ageing has already been observed by several authors in other tempered martensitic steels [23,30–32]. SEM observations (Fig. 11) clearly show the coalescence of carbides both after ageing at 600 °C for 1 h (Fig. 11b), and a fatigue test also performed at 600 °C (Fig. 11d). Conversely, the coalescence is obviously not observed after a fatigue test performed

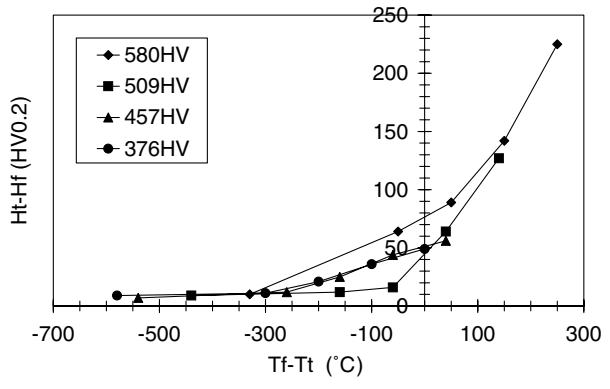

Fig. 9. Decrease in hardness versus difference between testing temperature (T_f) and tempering temperature (T_t).

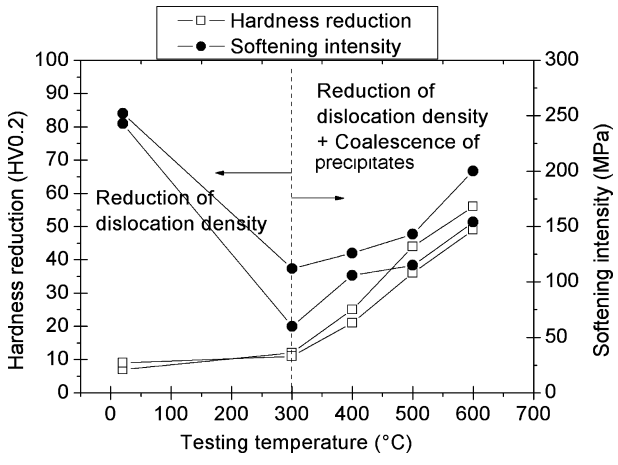

Fig. 10. Reduction in hardness and softening intensity versus the testing temperature.

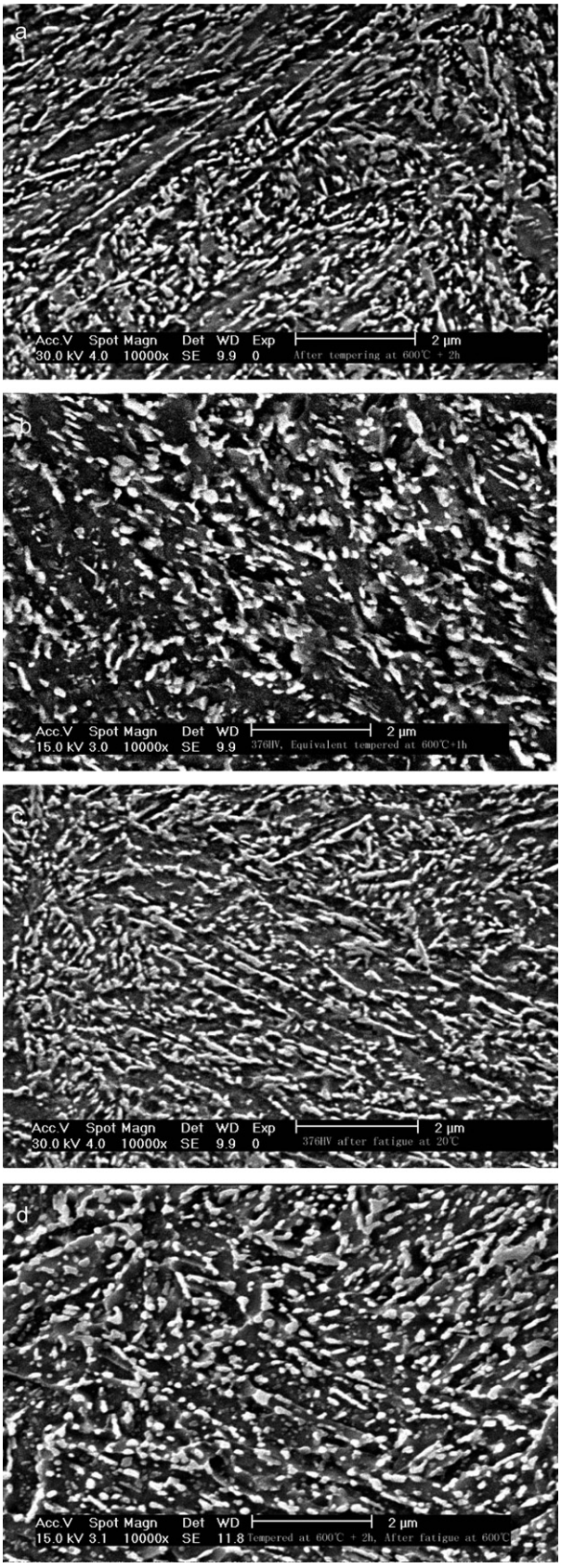

Fig. 11. SEM image of the population of iron carbides after: (a) a tempering at 600 °C for 2 h (376HV), (b) a tempering at 600 °C for 2 h and ageing at 600 °C for 1 h, (c) a tempering at 600 °C for 2 h and fatigue at 20 °C, (d) a tempering at 600 °C for 2 h and fatigue at 600 °C.

at 20 °C (Fig. 11c). Taking into account the above-mentioned considerations, the two parts of the curve of Fig. 10 can be explained as follows:

(i) At room temperature, only the sharp decrease of the dislocation density is observed inducing an intense cyclic softening as shown in Fig. 10. However, this mechanism can not be seen by hardness measurements, as a strong density of dislocations is introduced again during the indentation test. Therefore, the hardness level is only slightly modified at low temperatures.

(ii) Above 300 °C, cyclic softening results from both reduction of dislocation density and coalescence of iron carbides. The coalescence of carbides is not modified by the measurement performed at room temperature. Consequently, the hardness decrease observed above 300 °C (Fig. 10) should be connected primarily to the coalescence of carbides (Fig. 11), which is enhanced by both elevated temperature and mechanical loading [23].

In conclusion, the results clearly indicate the partial link between hardness variation and the real modification of the microstructure. The existing relationship between yield strength and hardness should be cautiously used when plasticity is involved during in-service conditions.

To investigate the effect of mechanical loads and thermal ageing on cyclic softening, some ageing tests were carried out for relevant temperatures and times corresponding to the fatigue test conditions. Comparison of hardness decreases observed during cyclic and ageing tests are shown in Fig. 12 for the specimens tempered at 350 °C. Results indicate that reduction in hardness can be divided into two parts: a thermal part due to thermal ageing and a mechanical part induced by cycling. The thermal part of reduction in hardness, predicted with the tempering kinetic law, has a good agreement with the decrease measured after an equivalent ageing test. Consequently, the tempering kinetic law can be used to predict the tempering ratio

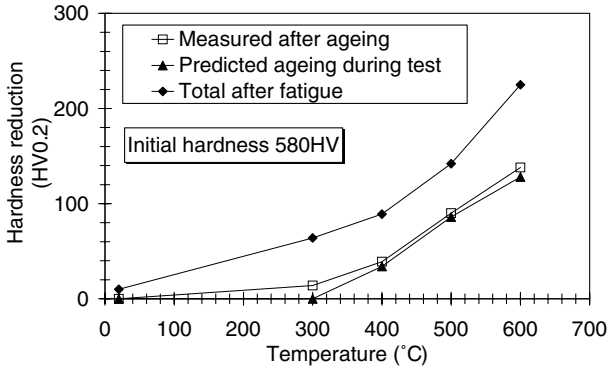

Fig. 12. Comparison between the hardness decrease measured after fatigue and ageing tests (same conditions of time and temperature) and the corresponding calculated value from Eq. (4).

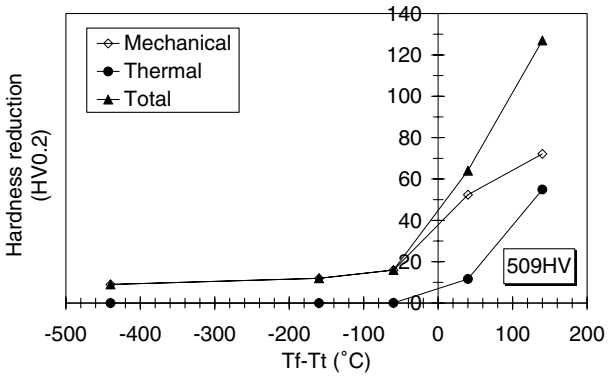

Fig. 13. Reduction in hardness according to the difference between testing temperature (T_f) and tempering temperature (T_t).

and to describe the steel evolution during tempering and ageing. Moreover, decomposition of the hardness decrease during fatigue can be discussed comparing hardness (tempering ratio) measurement and estimation. Fig. 13 shows an example of such decomposition for specimens with an initial hardness of 509HV. The decrease in hardness during fatigue entirely results from mechanical cycling when testing temperature is lower than tempering temperature. Reduction in hardness remains below 50HV. However, once the testing temperature exceeds the tempering temperature, hardness sharply decreases and the maximum value of hardness reduction can be as high as 225HV for a specimen with an initial hardness of 580HV. In that case, the reduction in hardness during fatigue can be divided into thermal and mechanical parts. Both thermal and mechanical hardness decreases with the difference between testing and tempering temperature.

As shown in Table 5 (bold underlined numbers), the tempering ratios increase when fatigue temperature is equal to or higher than the tempering temperature. In that case, an ageing of the steel is even stated during the 75 s before cycling (stabilisation time). So the kinetic law is able to predict the hardness evolution of the steel with time and temperature from the as-quenched state till the beginning of the fatigue test at elevated temperature. It would be useful to introduce this law in a cyclic behaviour model [11] as only one set of parameters would have to be identified for a large range of initial hardness (depending on the application). This work is in progress. Moreover, the ageing variation during cycling can be linked to the evolution of the steel towards the annealed state. However, the ageing parameter cannot predict the microstructural evolution at a nanometric scale during cycling.

5. Conclusion

Isothermal fatigue tests were carried out on a 55NiCrMoV7 steel to compare the ageing states obtained by the kinetic law described in [10] with the experimental data for different conditions of tempering and fatigue testing. Main results are summarised as follows:

(i) For testing temperatures lower than the tempering temperature, the maximum stress of the steel, as well as the stress amplitude measured at a constant cumulative plastic strain, increase with initial hardness and decrease with testing temperature. The ageing remains nearly constant.

(ii) Above the tempering temperature, a sharp ageing is observed even during the short time of the sample heating and temperature stabilisation stage before fatigue test starting. Moreover, the fatigue test clearly enhances the ageing of the steel (dynamic ageing).

(iii) Relation between cyclic softening and decrease in hardness during fatigue was investigated using Vickers hardness measurements. Results show a correct correlation at high temperature when carbides coalescence is one of the main softening mechanisms. However, the dynamic ageing (enhanced coalescence of carbides) cannot be predicted by the kinetic law. On the contrary, at the lowest temperatures of the experimental work, the hardness is only slightly modified during fatigue which is inconsistent with the sharp stress amplitude decrease measured with the testing machine. As the hardness measurement strongly modifies the dislocation structure and density, this test cannot describe the microstructural evolution when the rearrangement of dislocations generated by the quench is the main softening mechanism, which is obviously the case at low temperatures.

(iv) The hardness evolution of the steel is accurately predicted by the kinetic law from the as-quenched state till the beginning of the cyclic loading.

Acknowledgements

The authors gratefully acknowledge the Thyssen France Company for supplying the steel investigated and SRF for ROCS, SEM for financial support.

References

[1] Bernhart G, Moulinier G, Brucelle O, Delagnes D. High temperature low cycle fatigue behaviour of a martensitic forging tool steel. Int J Fatigue 1999;21(2):179–86.
[2] Bournicon C. Traitement Thermique 1991;246:70–7.
[3] Delagnes D. Isothermal fatigue behaviour and lifetime of a 5Cr hot work tool steel around the LCF–HCF transition. Ph.D. thesis, ENSMP; 1998 [in French].
[4] Komanduri R, Hou ZB. Int J Mech Sci 2001;43(1):57–88.
[5] Gibbons CL, Dunn JE. Ind Heat 1980:6–9.
[6] Zhang Z, Delagnes D, Bernhart G. Stress–strain behaviour of tool steels under thermo-mechanical loadings: experiments and modelling. In: Jeglitsch F, Ebner R, Leitner H, editors. Proceedings of the 5th international tooling conference. Austria: University of Leoben; 1999. p. 205–13.
[7] Velay V, Bernhart G, Zhang Z, Penazzi L. Cyclic behaviour modelling of martensitic hot work tool steels. In: Proceedings of

CAMP2002, high-temperature fatigue, Paderborn, Germany; 3–4 April 2002. p. 64–75.
[8] Bernhart G., Choi B.G., Zhang Z., Delagnes D. Single specimen methodology for elasto-visco-plastic fatigue model identification of martensitic steels. Euromat 2000, November, Tours, France. p. 1077–82.
[9] Zhang Z, Delagnes D, Bernhart G. Anisothermal cyclic plasticity modelling of martensitic steels. Int J Fatigue 2002;24(6): 635–48.
[10] Zhang Z, Delagnes D, Bernhart G. Microstructure evolution of hot-work tool steels during tempering and definition of a kinetic law based on hardness measurements. Mater Sci Eng A 2004;380 (1–2):222–30.
[11] Zhang Z. Anisothermal cyclic behaviour modelling with taking account of tempering effect of a martensitic tool steel 55NiCrMoV7. Ph.D. thesis, ENSMP; 2002 [in French].
[12] Zhang Z, Delagnes D, Bernhart G. Tempering effect on cyclic behaviour of a martensitic tool steel. In: Bergström J, Fredriksson G, Johansson M, kotik O, Thuvander F, editors. Proceedings of the 6th international tooling conference: the use of tool steels: experience and research, Karlstad University, Sweden. p. 573–89.
[13] Mutoh M, Okazaki Y. Low cycle fatigue strength and its prediction for dissimilar-metal electron-beam-welded joints at high temperature. In: Ohtani R, Ohnami M, Inoue T, editors. High temperature creep-fatigue. London, UK: Elsevier Applied Science; 1988. p. 183–202.
[14] Hiroyuki Okamura, Ryuichi Ohtani, Kiyoshi Saito. Nucl Eng Des 1999;193(3):243–54.
[15] Ye D, Tong X, Yao L. Mater Chem Phys 1998(56):199–204.
[16] Chen X, Zhao S-M. Evaluation of fatigue damage at welded tube joint under cyclic pressure using surface hardness measurement. Eng Fail Anal 2005;12:616–22.
[17] Mebarki N, Lamesle P, Delmas F, Delagnes D, Levaillant C. Relationship between microstructure and mechanical properties of a 5Cr hot-work tool steel. In: Bergström J, Fredriksson G, Johansson M, kotik O, Thuvander F, editors. Proceedings of the 6th international tooling conference: the use of tool steels: experience and research, Karlstad University, Sweden, p. 617–32.
[18] Mebarki N., Relationship between microstructure and mechanical properties of tempered martensitic steels. Ph.D. thesis, ENSMP; 2003 [in French].
[19] Lemaitre J, Chaboche JL. Mechanics of solids. Cambridge University Press; 1990.
[20] Francois D, Pineau A, Zaoui A. Comportement mécanique des matériaux–viscoplasticité, endommagement, mécanique de la rupture, mécanique du contact. Paris: HERMES; 1993.
[21] Pesicka J, Kuzel R, Dronhofer A, Eggeler G. The evolution of dislocation density during heat treatment and creep of tempered martensite ferritic steels. Acta Mater 2003;51(16):4847–62.
[22] Pesicka J, Dronhofer A, Eggeler G. Free dislocations and boundary dislocations in tempered martensite ferritic steels. Mater Sci Eng A 2004;387–389(1–2):176–80.
[23] Delagnes D, Lamesle P, Mathon MH, Mebarki N, Levaillant C. Influence of silicon content on the precipitation of secondary carbides and fatigue properties of a 5%Cr tempered martensitic steel. Mater Sci Eng A 2005;394(1–2):435–44.
[24] Mebarki N, Delagnes D, Lamesle P, Delmas F, Levaillant C. Relationship between microstructure and mechanical properties of a 5%Cr tempered martensitic tool steel. Mater Sci Eng A 2004;387–389(1–2):171–5.
[25] Hu Z, Xiao J. Cyclic softening characteristics and mechanism of hot work die steels during low cycle fatigue. In: Fatigue '90, Proceedings of the 4th international conference on fatigue and fatigue thresholds, Honolulu; 1990. p. 469–74.
[26] Kanazawa K, Yamaguchi K, Kobayashi K. The temperature dependence of low cycle fatigue behaviour of martensitic stainless steels. Mater Sci Eng 1979;40:89–96.
[27] Vogt JB, Degallaix G, Foct J. Cyclic mechanical behaviour and microstructure of a 12Cr–Mo–V martensitic stainless steel. Fatigue Fract Eng Mater Struct 1988;11:435–46.
[28] Vogt JB, Argillier S, Leon J, Massoud JP, Prunier V. Mechanisms of cyclic plasticity of a ferrite–bainite 21/4Cr1Mo steel after long-term service at high temperature. ISIJ Int 1999;39:1198–203.
[29] Chai H, Fan Q. fatigue softening mechanism of low carbon tempered martensite. In: Fatigue '93, Proceedings of the 5th international conference on fatigue and fatigue thresholds, Montreal; 1993. p. 195–200.
[30] Eggeler G. The effect of long-term creep on particle coarsening in tempered martensite ferritic steels. Acta Metall 1989;37(12):3225–34.
[31] Chang HJ, Tsai CH, Kai JJ. Effects of temperature on the cyclic deformation behaviour and microstructural changes of 12Cr–1MoVW martensitic stainless steel. Int J Pres Ves Pip 1994;59(1–3): 31–40.
[32] Wang ZG, Rahka K, Nenonen P, Laird C. Changes in morphology and composition of carbides during cyclic deformation at room and elevated temperature and their effect on mechanical properties of Cr–Mo–V steel. Acta Metall 1985;33:2129–41.